

The heavy-quark hybrid meson spectrum in lattice QCD

K. Jimmy Juge*, Julius Kuti† and Colin Morningstar**

**Institute for Theoretical Physics, University of Bern, Sidlerstrasse 5, CH-3012 Bern, Switzerland*

†*Department of Physics, University of California at San Diego, La Jolla, USA 92093-0319*

***Department of Physics, Carnegie Mellon University, Pittsburgh, PA, USA 15213-3890*

Abstract. Recent findings on the spectrum of heavy-quark mesons from computer simulations of quarks and gluons in lattice QCD are summarized, with particular attention to quark-antiquark states bound by an excited gluon field. The validity of a Born-Oppenheimer treatment for such systems is discussed. Recent results on glueball masses, the light-quark 1^{-+} hybrid meson mass, and the static three-quark potential are summarized.

INTRODUCTION

Much of our current understanding of hadron formation comes from the constituent quark model. The quark model is motivated by quantum chromodynamics (QCD) and views hadrons as valence quarks interacting via an instantaneous confining Coulomb plus linear potential. In the quark model, the gluons are recognized as the source of the confining potential, but their dynamics is completely ignored.

Most of the observed hadron spectrum is described reasonably well by the quark model. The agreement is remarkable given the crudeness of the model. In the quark model, mesons may have only certain J^{PC} quantum numbers: if the total spin and orbital angular momentum of the quark-antiquark pair are $S = 0, 1$ and $L = 0, 1, 2, \dots$, respectively, then the parity and charge conjugation are given by $P = (-1)^{L+1}$ and $C = (-1)^{L+S}$. In other words, $0^{+-}, 0^{-+}, 1^{-+}, 2^{+-}, 3^{-+}, 4^{+-}, \dots$ are forbidden and mesons having such J^{PC} are known as exotics. Both an overabundance of observed states and recent observations of exotic 1^{-+} resonances[1] underscore the need to understand hadron formation beyond the quark model.

QCD suggests the existence of states in which the gluon field is excited. Such states with no valence quark content are termed glueballs, whereas states consisting of a valence quark-antiquark pair or three valence quarks bound by an excited gluon field are known as hybrid mesons and hybrid baryons, respectively. Glueballs and hybrids are currently not well understood, making their experimental identification difficult. Theoretical investigations into their nature must confront the long-standing problem of dealing with nonperturbative gluon field behavior, but for this reason, such states are a potentially rich source of information concerning the confining properties of QCD.

In this talk¹, progress in understanding heavy-quark conventional and hybrid mesons using lattice simulations of gluons is reported. The validity of a Born-Oppenheimer treatment of such systems is discussed. Results on glueball masses, the light quark 1^{-+} hybrid meson mass, and the static three-quark potential are also summarized.

HEAVY-QUARK HYBRID MESONS

The study of heavy-quark mesons is a natural starting point in the search to understand hadron formation. The vastly different characteristics of the slow massive heavy quarks and the fast massless gluons suggest that such systems may be amenable to a Born-Oppenheimer treatment, similar to diatomic molecules[2]. The slow heavy quarks correspond to the nuclei in diatomic molecules, whereas the fast gluon and light-quark fields correspond to the electrons. One expects that the gluon/light-quark wavefunctionals adapt nearly instantaneously to changes in the heavy quark-antiquark separation. At leading order, the gluons and light quarks provide adiabatic potentials $V_{Q\bar{Q}}(r)$ which can be computed in lattice simulations. The leading order behavior of the heavy quarks is then described by solving the Schrödinger equation separately for each $V_{Q\bar{Q}}(r)$:

$$\left\{ \frac{\mathbf{p}^2}{2\mu} + V_{Q\bar{Q}}(r) \right\} \Psi_{Q\bar{Q}}(r) = E \Psi_{Q\bar{Q}}(r), \quad (1)$$

where μ is the reduced mass of the quark-antiquark pair and r is the quark-antiquark separation. The Born-Oppenheimer approximation provides a clear and unambiguous picture of conventional and hybrid mesons: conventional mesons arise from the lowest-lying adiabatic potential, whereas hybrid mesons arise from the excited-state potentials. The validity of such a Born-Oppenheimer picture will be demonstrated in this talk.

Excitations of the static quark potential

The first step in a Born-Oppenheimer treatment of heavy quark mesons is determining the gluonic terms $V_{Q\bar{Q}}(r)$. Since familiar Feynman diagram techniques fail and the Schwinger-Dyson equations are intractable, the path integrals needed to determine $V_{Q\bar{Q}}(r)$ are usually estimated using Markov-chain Monte Carlo methods. The spectrum of gluonic excitations in the presence of a static quark-antiquark pair has been accurately determined in recent lattice simulations[3, 4, 5] which make use of anisotropic lattices, improved actions, and large sets of operators with correlation matrix techniques.

The results for one particular lattice spacing are shown in Fig. 1. Due to computational limitations, light quark loops have been neglected in these calculations; their expected impact on the meson spectrum will be discussed below. The levels in Fig. 1 are labeled by the magnitude Λ of the projection of the total angular momentum \mathbf{J}_g of the gluon field onto the molecular axis, and by $\eta = \pm 1$, the symmetry under charge conjugation

¹ Presented by C. Morningstar.

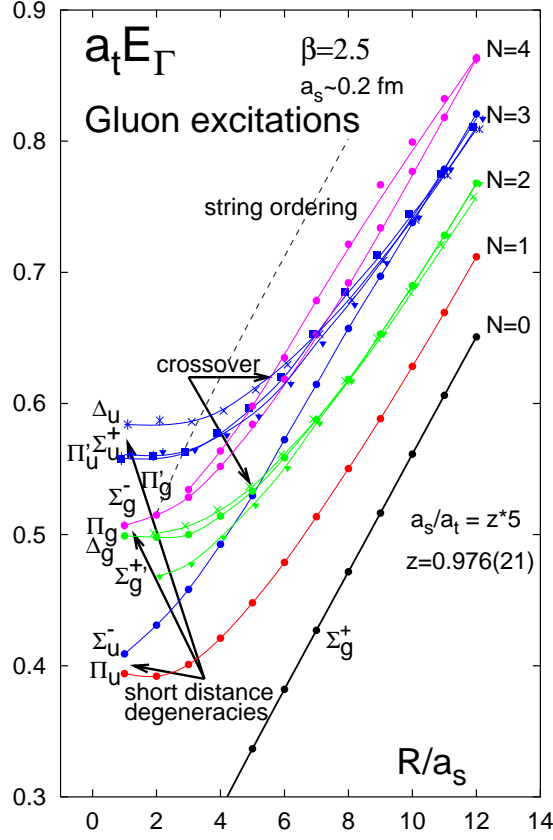


FIGURE 1. The spectrum of gluonic excitations in the presence of a static quark-antiquark pair from Ref. [5]. The solid curves are only shown for visualization. At short distances, the level orderings and degeneracies are consistent with the states expected in a multipole operator product expansion. At large distances, the levels are consistent with the expectations from an effective string theory description. A dramatic level rearrangement is observed in the crossover region between 0.5 – 2.0 fm. The dashed line marks a lower bound for the onset of mixing effects with glueball states which requires careful interpretation.

combined with spatial inversion about the midpoint between the Q and \bar{Q} . States with $\Lambda = 0, 1, 2, \dots$ are denoted by $\Sigma, \Pi, \Delta, \dots$, respectively. States which are even (odd) under the above-mentioned CP operation are denoted by the subscripts g (u). An additional \pm superscript for the Σ states refers to even or odd symmetry under a reflection in a plane containing the molecular axis.

These $V_{Q\bar{Q}}(r)$ potentials tell us much about the nature of the confining gluon field between a quark and an antiquark. Innumerable lattice QCD simulations have confirmed the linearly rising ground-state static quark-antiquark potential from gluon exchange. Such a linearly rising potential naively suggests that the gluon field forms a string-like confining object connecting the quark and the antiquark. However, it should be noted that the spherical bag model also predicts a linearly rising potential for moderate r , and hence, the linearly rising ground-state potential is *not* conclusive evidence of string formation. Computations of the gluon action density surrounding a static quark-

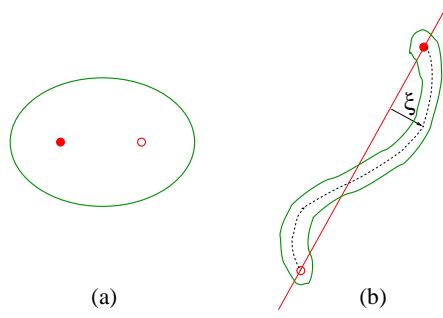


FIGURE 2. One possible interpretation of the spectrum in Fig. 1. (a) For small quark-antiquark separations, the strong chromoelectric field of the $Q\bar{Q}$ pair repels the physical vacuum (dual Meissner effect) creating a bubble. The low-lying stationary states are explained by the gluonic modes inside the bubble, since the bubble surface excitations are likely to be higher lying. (b) For large quark-antiquark separations, the bubble stretches into a thin tube of flux, and the low-lying states are explained by the collective motion of the tube since the internal gluonic excitations are much higher lying.

antiquark pair in $SU(2)$ gauge theory also hint at flux tube formation[6].

The spectrum shown in Fig. 1 provides unequivocal evidence that the gluon field can be well approximated by an effective string theory for large separations r . However, string formation does not appear to set in until the quark and the antiquark are separated by about 2 fm. For small separations, the level orderings and degeneracies are not consistent with the expectations from an effective string description. More importantly, the gaps differ appreciably from $N\pi/r$ with $N = 1, 2, 3, \dots$. Such deviations cannot be considered mere corrections, making the applicability of an effective string description problematical. Between 0.5 to 2 fm, a dramatic level rearrangement occurs. For separations above 2 fm, the levels agree *without exception* with the ordering and degeneracies expected from an effective string theory. The gaps agree well with $N\pi/r$, but a fine structure remains. The $N\pi/r$ gaps are a robust prediction of any effective string theory since they are a feature of the Goldstone modes associated with the spontaneous breaking of transverse translational symmetry. However, the details of the underlying string theory are encoded in the fine structure. This first glimpse of such a fine structure offers the exciting possibility of ultimately understanding the nature of the QCD string in future higher precision simulations.

Fig. 2 illustrates one possible interpretation of the results shown in Fig. 1. At small quark-antiquark separations, the strong chromoelectric field of the $Q\bar{Q}$ pair repels the physical vacuum in a dual Meissner effect, creating a bubble surrounding the $Q\bar{Q}$. The low-lying stationary states are explained by the gluonic modes inside the bubble, since the bubble surface excitations are likely to be higher lying. For large quark-antiquark separations, the bubble stretches into a thin tube of flux, and the low-lying states are explained by the collective motion of the tube since the internal gluonic excitations, being typically of order 1 GeV, are now much higher lying.

The leading Born-Oppenheimer approximation

In the leading Born-Oppenheimer approximation, one replaces the covariant Laplacian \mathbf{D}^2 by an ordinary Laplacian ∇^2 , which neglects retardation effects. The spin interactions of the heavy quarks are also neglected, and one solves the radial Schrödinger equation:

$$-\frac{1}{2\mu} \frac{d^2 u(r)}{dr^2} + \left\{ \frac{\langle \mathbf{L}_{Q\bar{Q}}^2 \rangle}{2\mu r^2} + V_{Q\bar{Q}}(r) \right\} u(r) = E u(r), \quad (2)$$

where $u(r)$ is the radial wavefunction of the quark-antiquark pair. The total angular momentum is given by

$$\mathbf{J} = \mathbf{L} + \mathbf{S}, \quad \mathbf{S} = \mathbf{s}_Q + \mathbf{s}_{\bar{Q}}, \quad \mathbf{L} = \mathbf{L}_{Q\bar{Q}} + \mathbf{J}_g, \quad (3)$$

where \mathbf{s}_Q is the spin of the heavy quark, $\mathbf{s}_{\bar{Q}}$ is the spin of the heavy antiquark, \mathbf{J}_g is the total spin of the gluon field, and $\mathbf{L}_{Q\bar{Q}}$ is the orbital angular momentum of the quark-antiquark pair. In the LBO, both L and S are good quantum numbers. The expectation value in the centrifugal term is given by

$$\langle \mathbf{L}_{Q\bar{Q}}^2 \rangle = \langle \mathbf{L}^2 \rangle - 2\langle \mathbf{L} \cdot \mathbf{J}_g \rangle + \langle \mathbf{J}_g^2 \rangle. \quad (4)$$

The first term yields $L(L+1)$. The second term is evaluated by expressing the vectors in terms of components in the body-fixed frame. Let L_r denote the component of \mathbf{L} along the molecular axis, and L_ξ and L_ζ be components perpendicular to the molecular axis. Writing $L_\pm = L_\xi \pm iL_\zeta$ and similarly for \mathbf{J}_g , one obtains

$$\langle \mathbf{L} \cdot \mathbf{J}_g \rangle = \langle L_r J_{gr} \rangle + \frac{1}{2} \langle L_+ J_{g-} + L_- J_{g+} \rangle. \quad (5)$$

Since $J_{g\pm}$ raises or lowers the value of Λ , this term mixes different gluonic stationary states, and thus, must be neglected in the leading Born-Oppenheimer approximation. In the meson rest frame, the component of $\mathbf{L}_{Q\bar{Q}}$ along the molecular axis vanishes, and hence, $\langle L_r J_{gr} \rangle = \langle J_{gr}^2 \rangle = \Lambda^2$. In summary, the expectation value in the centrifugal term is given in the adiabatic approximation by

$$\langle \mathbf{L}_{Q\bar{Q}}^2 \rangle = L(L+1) - 2\Lambda^2 + \langle \mathbf{J}_g^2 \rangle. \quad (6)$$

We assume $\langle \mathbf{J}_g^2 \rangle$ is saturated by the minimum number of allowed gluons. Hence, $\langle \mathbf{J}_g^2 \rangle = 0$ for the Σ_g^+ level and $\langle \mathbf{J}_g^2 \rangle = 2$ for the Π_u and Σ_u^- levels. Wigner rotations are used as usual to construct $|LSJM; \lambda \eta\rangle$ states, where $\lambda = \mathbf{J}_g \cdot \hat{\mathbf{r}}$ and $\Lambda = |\lambda|$, then J^{PC} eigenstates are finally obtained from

$$|LSJM; \lambda \eta\rangle + \varepsilon |LSJM; -\lambda \eta\rangle, \quad (7)$$

where $\varepsilon = 1$ for Σ^+ levels, $\varepsilon = -1$ for Σ^- levels, and $\varepsilon = \pm 1$ for $\Lambda \geq 1$ levels. Hence, the J^{PC} eigenstates satisfy

$$P = \varepsilon (-1)^{L+\Lambda+1}, \quad C = \eta \varepsilon (-1)^{L+S+\Lambda}. \quad (8)$$

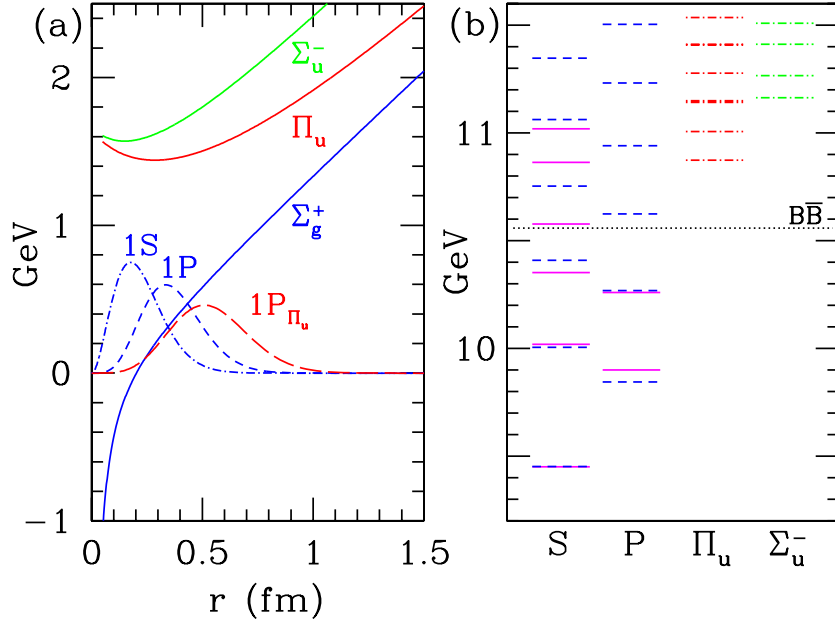


FIGURE 3. (a) Static potentials and radial probability densities against quark-antiquark separation r for the conventional $1S$ and $1P$ bottomonium states and the hybrid $1P_{\Pi_u}$ level. The scale is set using $r_0^{-1} = 450$ MeV. (b) Spin-averaged spectrum in the LBO approximation (light quarks neglected). Solid lines indicate experimental measurements. Short dashed lines indicate the S and P state masses obtained using the Σ_g^+ potential with $M_b = 4.58$ GeV. Dashed-dotted lines indicate the hybrid quarkonium states obtained from the Π_u ($L = 1, 2, 3$) and Σ_u^- ($L = 0, 1, 2$) potentials. These results are from Ref. [7].

Note that many levels are degenerate in the LBO approximation:

$$\begin{aligned}
 \Sigma_g^+(S) &: 0^{-+}, 1^{--}, \\
 \Sigma_g^+(P) &: 0^{++}, 1^{++}, 2^{++}, 1^{+-}, \\
 \Pi_u(P) &: 0^{-+}, 0^{+-}, 1^{++}, 1^{--}, 1^{+-}, 1^{-+}, 2^{+-}, 2^{-+}.
 \end{aligned}$$

The LBO spectrum[7] of conventional $\bar{b}b$ and hybrid $\bar{b}gb$ states is shown in Fig. 3. Below the $B\bar{B}$ threshold, the LBO results agree well with the spin-averaged experimental measurements of bottomonium states (any small discrepancies disappear once light quark loops are included). Above the threshold, agreement with experiment is lost, suggesting significant corrections either from mixing and other higher-order effects or (more likely) from light sea quark effects. Note from the radial probability densities shown in Fig. 3 that the size of the hybrid state is large in comparison with the conventional $1S$ and $1P$ states. The analogous results in charmonium are shown in Fig. 4.

The validity of such a simple physical picture relies on the smallness of higher-order spin, relativistic, and retardation effects, as well as mixings between states based on different $V_{Q\bar{Q}}(r)$. The importance of retardation and leading-order mixings between states based on different adiabatic potentials was tested in Ref. [7] by comparing the LBO level splittings with those determined from meson simulations using a leading-order non-relativistic (NRQCD) heavy-quark action. The NRQCD action included only a covariant temporal derivative and the leading covariant kinetic energy operator; quark spin and D^4 terms were neglected. The simulations include retardation effects and allow

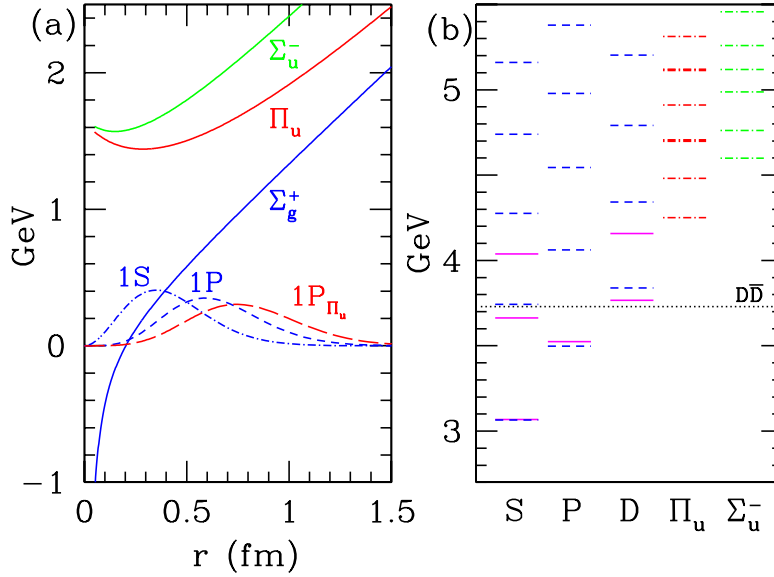


FIGURE 4. (a) Static potentials and radial probability densities against quark-antiquark separation r with $r_0^{-1} = 415$ MeV for the conventional $1S$ and $1P$ charmonium levels and the hybrid $1P_{\Pi_u}$ state. (b) Spin-averaged spectrum in the LBO approximation (light quarks neglected). Solid lines indicate experimental measurements. Short dashed lines indicate the $S, P,$ and D state masses obtained using the Σ_g^+ potential with $M_c = 1.20$ GeV. Dashed-dotted lines indicate the hybrid quarkonium states obtained from the Π_u ($L = 1, 2, 3$) and Σ_u^- ($L = 0, 1, 2$) potentials.

TABLE 1. The meson spin-singlet operators used in the simulations of Ref. [7] in terms of the heavy quark two-component field ψ , antiquark field χ , covariant derivative \mathbf{D} , and chromomagnetic field \mathbf{B} . Note that $p = 0, 1, 2,$ and 3 were used to produce four distinct operators in the 0^{-+} and 1^{-+} sectors. In the third column are listed the spin-triplet states which can be formed from the operators in the last column; the states in each row are degenerate for the NRQCD action used here.

J^{PC}		Degeneracies	Operator
0^{-+}	S wave	1^{-+}	$\chi^\dagger (\mathbf{D}^2)^p \psi$
1^{+-}	P wave	$0^{++}, 1^{++}, 2^{++}$	$\chi^\dagger \mathbf{D} \psi$
1^{-+}	H_1 hybrid	$0^{-+}, 1^{-+}, 2^{-+}$	$\chi^\dagger \mathbf{B} (\mathbf{D}^2)^p \psi$
1^{+-}	H_2 hybrid	$0^{+-}, 1^{+-}, 2^{+-}$	$\chi^\dagger \mathbf{B} \times \mathbf{D} \psi$
0^{++}	H_3 hybrid	1^{+-}	$\chi^\dagger \mathbf{B} \cdot \mathbf{D} \psi$

possible mixings between different adiabatic surfaces. The level splittings (in terms of the hadronic scale r_0 and with respect to the $1S$ state) of the conventional $2S$ and $1P$ states and four hybrid states were compared (see Fig. 5) and found to agree within 10%, strongly supporting the validity of the leading Born-Oppenheimer picture. The operators used to create the mesons in the simulations are described in Table 1.

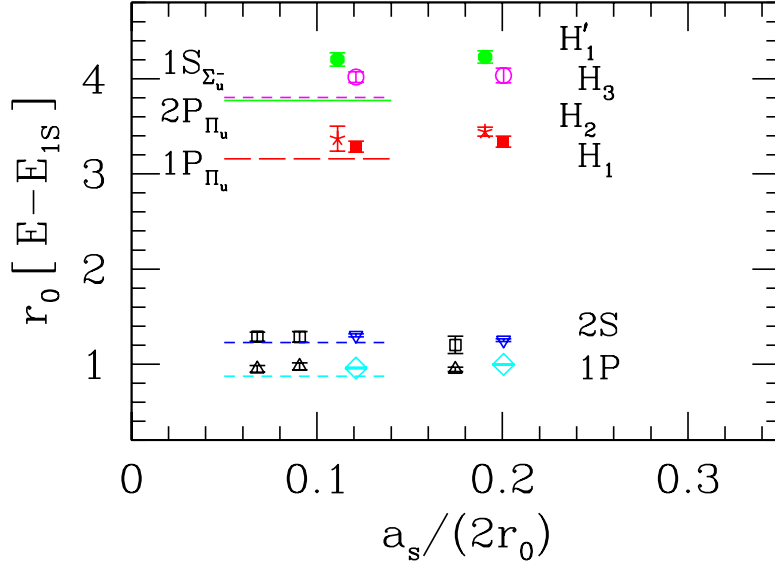


FIGURE 5. Simulation results from Ref. [7] for the heavy quarkonium level splittings of two conventional levels and four hybrid levels (in terms of r_0 and with respect to the $1S$ state) against the lattice spacing a_s . Results from Ref. [8] using an NRQCD action with higher-order corrections are shown as open boxes and \triangle . The horizontal lines show the LBO predictions. Agreement of these splittings within 10% validates the leading Born-Oppenheimer approximation (in the absence of light quarks).

Quark spin effects and light-quark loops

A very recent study[9] has shown that heavy-quark spin effects are unlikely to spoil the Born-Oppenheimer approximation. Using lowest-order lattice NRQCD to create heavy-quark propagators, a basis of unperturbed S -wave and $|1H\rangle$ hybrid states were formed. The $c_B \boldsymbol{\sigma} \cdot \mathbf{B} / 2M_Q$ spin interaction was then applied at an intermediate time slice to compute the mixings between such states due to this interaction in the quenched approximation (see Fig. 6). For a reasonable range of c_B values, the following results were obtained:

$$\begin{aligned} \langle 1H | \Upsilon \rangle &\approx 0.076 - 0.11, & \langle 1H | J/\Psi \rangle &\approx 0.18 - 0.25, \\ \langle 1H | \eta_b \rangle &\approx 0.13 - 0.19, & \langle 1H | \eta_c \rangle &\approx 0.29 - 0.4. \end{aligned}$$

Hence, mixings due to quark spin effects in bottomonium are very small, and even in charmonium, the mixings are not large.

In the absence of light quark loops, one obtains a very dense spectrum of mesonic states since the $V_{Q\bar{Q}}(r)$ potentials increase indefinitely with r . However, the inclusion of light quark loops changes the $V_{Q\bar{Q}}(r)$ potentials. First, there are slight corrections at small r , and these corrections remove the small discrepancies of the LBO predictions with experiment below the $B\bar{B}$ threshold seen in Fig. 3. For large r , the inclusion of light quark loops drastically changes the behavior of the $V_{Q\bar{Q}}(r)$ potentials: instead of increasing indefinitely, these potentials eventually level off at a separation above 1 fm when the static quark-antiquark pair, joined by gluonic flux, can undergo fission into $(Q\bar{q})(\bar{Q}q)$, where q is a light quark. Clearly, such potentials cannot support the

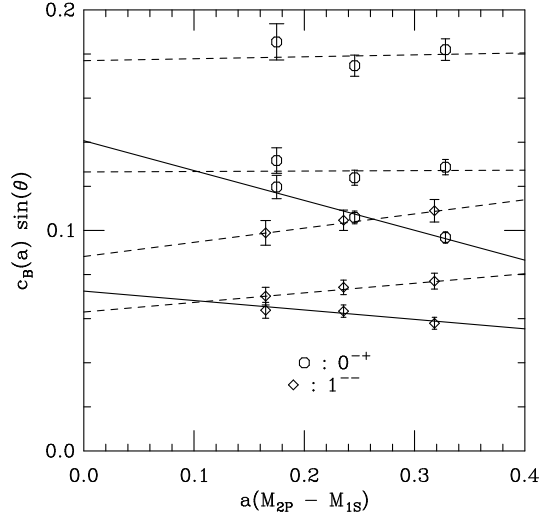


FIGURE 6. Hybrid/ S -wave configuration mixing angle against lattice spacing. For each channel, the lowest three points with solid fit line reflect tree-level values for c_B , and the higher two sets of three points result from setting c_B using 30 and 60 MeV for the S -wave hyperfine splitting.

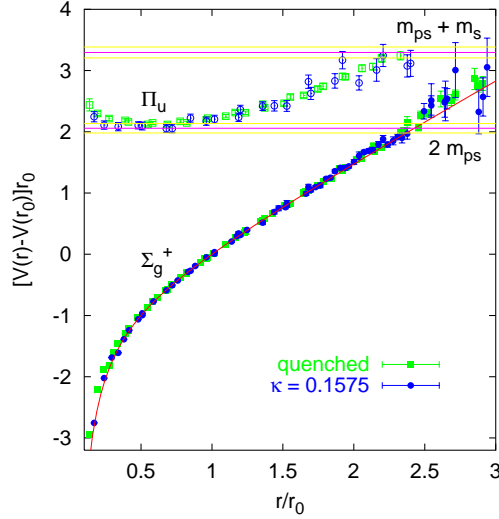


FIGURE 7. Ground Σ_g^+ and first-excited Π_u static quark potentials without sea quarks (squares, quenched) and with two flavors of sea quarks, slightly lighter than the strange quark (circles, $\kappa = 0.1575$). Results are given in terms of the scale $r_0 \approx 0.5$ fm, and the lattice spacing is $a \approx 0.08$ fm. Note that m_S and m_{PS} are the masses of a scalar and pseudoscalar meson, respectively, consisting of a light quark and a static antiquark. These results are from Ref. [10].

populous set of states shown in Fig. 3; the formation of bound states and resonances substantially extending over 1 fm in diameter seems unlikely. A complete open-channel calculation taking the effects of including the light quarks correctly into account has not yet been done, but unquenched lattice simulations[10] show that the Σ_g^+ and Π_u potentials change very little for separations below 1 fm when sea quarks are included

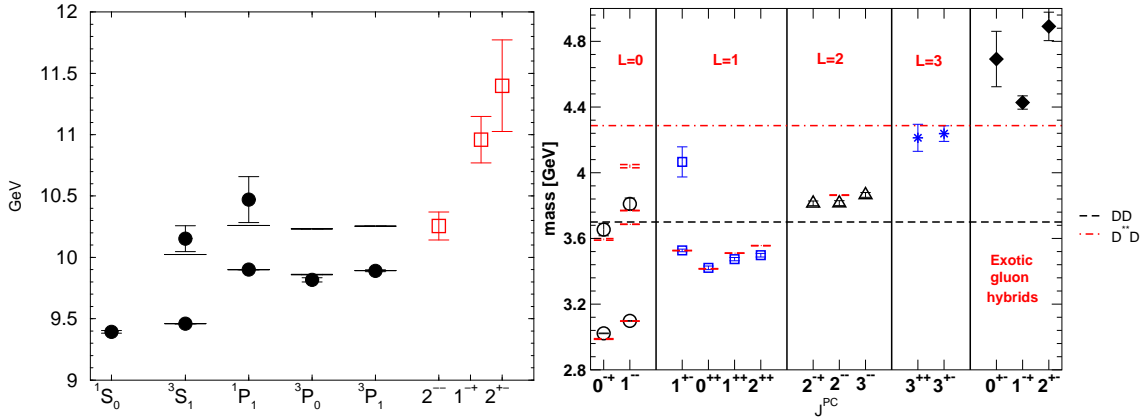


FIGURE 8. The bottomonium spectrum (left) from Ref. [11] and charmonium spectrum (right) from Ref. [12] in the quenched approximation using an anisotropic clover fermion action. The $^1P_1 - ^3S_1$ splitting is used to set the scale. Experimental values are indicated by the horizontal lines. In the $b\bar{b}$ spectrum, the two rightmost points indicate exotic hybrid candidates which agree with the Born-Oppenheimer predictions, but with very large uncertainties. In the $c\bar{c}$ spectrum, the three rightmost points indicate results for hybrid candidates.

(see Fig. 7), suggesting that a handful of low-lying states whose wavefunctions do not extend appreciably beyond 1 fm in diameter may exist as well-defined resonances in nature.

Simulations with relativistic heavy quarks

A recent quenched calculation[11] of bottomonium hybrids using a relativistic heavy-quark action on anisotropic lattices confirms the predictions of the Born-Oppenheimer approximation, but admittedly, the uncertainties in the simulation results are large (see Fig. 8). These calculations make use of a Symanzik-improved anisotropic gauge action and an improved fermion clover action. These same authors have also recently studied the charmonium spectrum[12]. The results, shown in Fig. 8, suggest significant, but not large, corrections to the leading Born-Oppenheimer approximation.

OTHER TIDBITS

Some other recent studies involving gluonic excitations are summarized in the remainder of this talk.

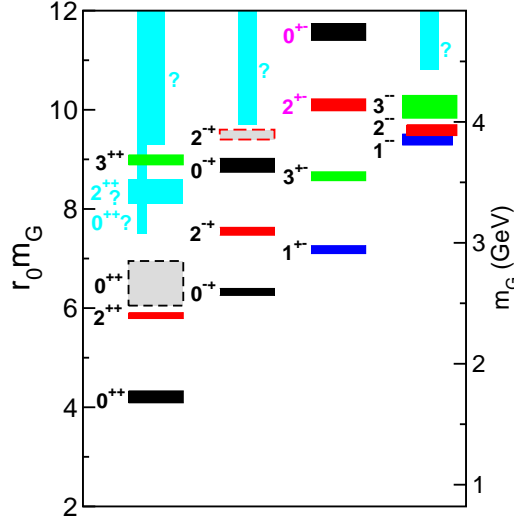


FIGURE 9. The mass spectrum of glueballs in the pure SU(3) gauge theory from Ref. [13]. The masses are given in terms of the hadronic scale r_0 along the left vertical axis and in terms of GeV along the right vertical axis (assuming $r_0^{-1} = 410(20)$ MeV). The mass uncertainties indicated by the vertical extents of the boxes do *not* include the uncertainty in setting r_0 . The locations of states whose interpretation requires further study are indicated by the dashed hollow boxes. The shaded strips with accompanying question marks indicate regions in which the spectrum is not known.

Glueballs

The glueball spectrum in the absence of virtual quark-antiquark pairs is now well known[13] and is shown in Fig. 9. The glueball spectrum can be qualitatively understood in terms of the interpolating operators of minimal dimension which can create glueball states[14] and can be reasonably well explained[15] in terms of a simple constituent gluon (bag) model which approximates the gluon field using spherical cavity Hartree modes with residual perturbative interactions[16, 17], as shown in Fig. 10. This figure also shows that a model[18] of glueballs as loops of chromoelectric flux completely fails to explain the spectrum.

Light-quark exotic 1^{-+} hybrid meson

There are recent new determinations of the exotic 1^{-+} meson mass[19] using improved staggered fermions and the Wilson gluon action at a lattice spacing $a \approx 0.09$ fm. Both quenched ($n_f = 0$) and unquenched ($n_f = 2 + 1, 3$) simulation results are presented. The $n_f = 3$ and $n_f = 2 + 1$ simulation differ in how the three quark mass parameters m_u , m_d , and m_s were chosen. In the $n_f = 3$ simulations, $m_u = m_d = m_s$ near the strange quark mass was used, and in the $n_f = 2 + 1$ simulations, $m_u = m_d = 0.4m_s$ was used. The results are compared to previous determinations in Fig. 11 and remain somewhat heavier than the experimental candidates.

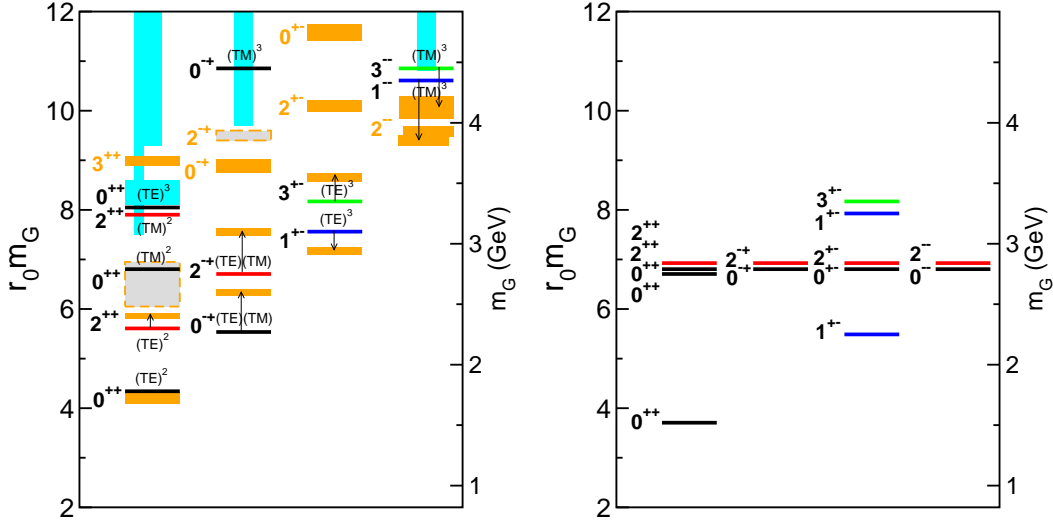


FIGURE 10. Comparison of the glueball spectrum obtained from Monte Carlo simulations with that predicted by the bag model (left) with $\alpha_s = 0.5$ and $B^{1/4} = 280$ MeV, and the Isgur-Paton flux tube model (right). The crude bag model appears to capture the qualitative features of the spectrum, whereas the flux tube model fails entirely. The bag model results shown above do not include gluon self-energies, but the incorporation of such contributions is not expected to change the spectrum appreciably.

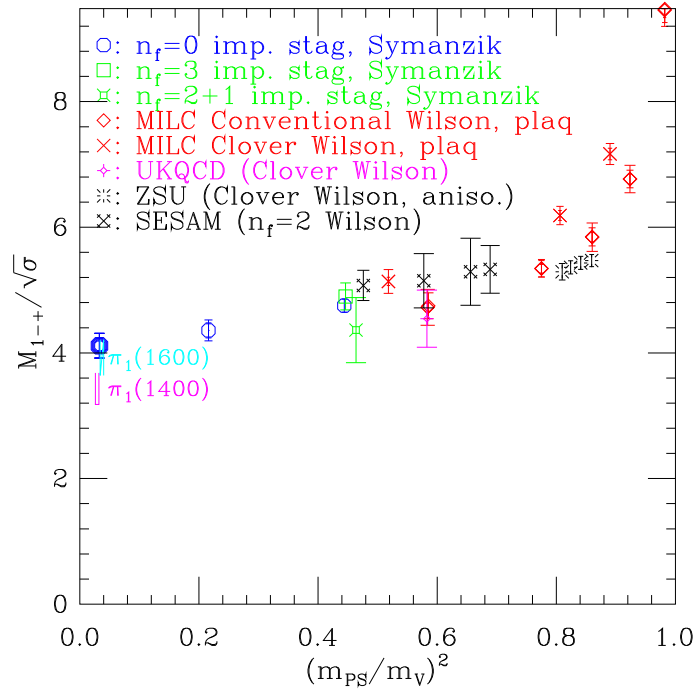


FIGURE 11. Summary of recent determinations of the 1^{-+} hybrid meson mass against $(m_{PS}/m_V)^2$. The bold octagon indicates a linear extrapolation of quenched $n_f = 0$ results to the physical point $(m_{PS}/m_V)^2 = 0.033$. The most recent results make use of improved staggered fermions[19] and remain somewhat heavier than the experimental candidates.

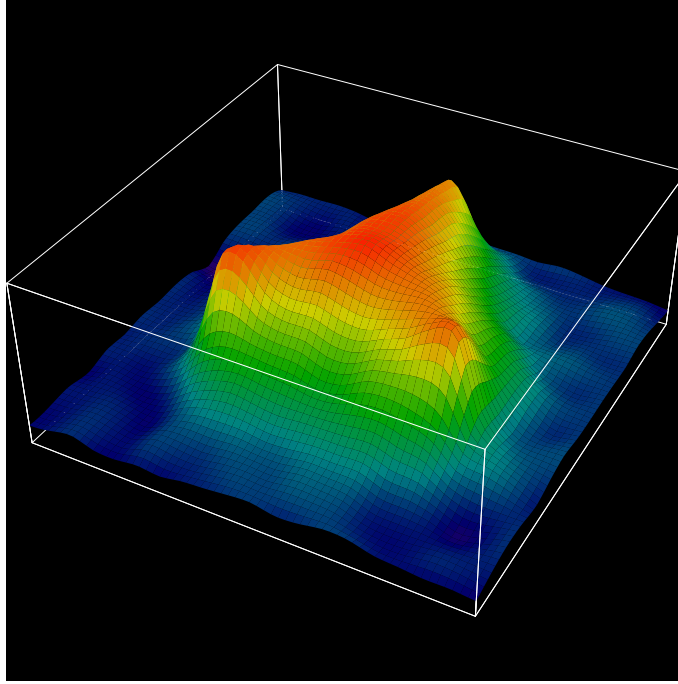


FIGURE 12. The abelian action density of gluons in the presence of three static quarks from Ref. [20]. These results support the so-called Y ansatz, and were obtained using the Wilson gauge action with $\beta = 6.0$ (lattice spacing $a \sim 0.1$ fm) on a $16^3 \times 32$ lattice. The three static quarks were located at sites $(17, 14)$, $(22, 6)$, and $(12, 6)$ in the xy -plane. A calculation in Ref. [21] including light quark loops shows similar results.

Static three-quark potential

The behavior of gluons in the presence of three static quarks has come under recent study and promises to shed light on the structure of baryons. In Ref. [20], the abelian action density of gluons in the presence of three static quarks has been calculated and is shown in Fig. 12. The results favor a Y -ansatz in which the quarks are confined by a genuine three-body force consisting of three gluonic fluxes meeting at a common junction. An alternative Δ -ansatz composed of three sets of two-body interactions is disfavored. A calculation in Ref. [21] which includes light sea quarks shows similar results.

The first excitation of gluons in the presence of three static quarks has also recently been studied[22]. The results are shown in Fig. 13. Although systematic uncertainties from finite lattice spacing and finite volume still need to be investigated, the results indicate an excitation energy near 1 GeV.

CONCLUSION

Hadronic states bound by an excited gluon field are an interesting new form of matter. Theoretical investigations into their nature must confront the long-standing problem of

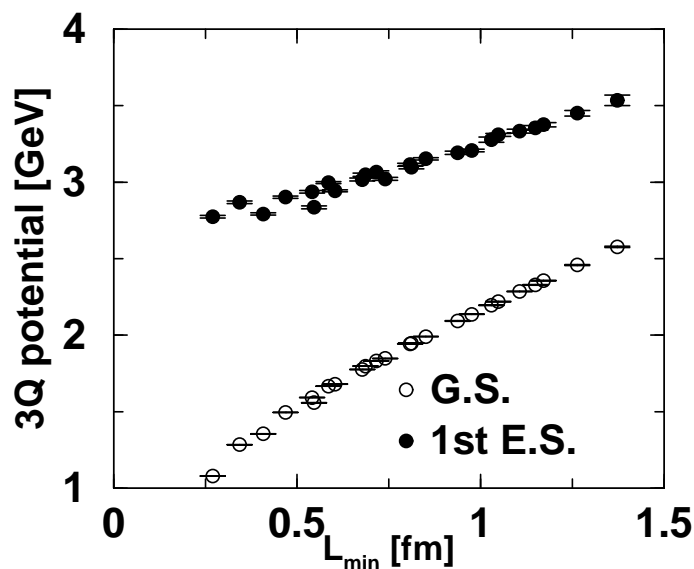


FIGURE 13. Energies of the ground and first-excited stationary states of gluons in the presence of three static quarks against L_{\min} , the minimal total length of three line segments connecting the three quarks at a common junction. The scale is set using the string tension $\sigma = 0.89$ GeV/fm. These results are from Ref. [22] and were obtained using the Wilson gauge action at $\beta = 5.8$ on a $16^3 \times 32$ lattice.

understanding the confining gluon field, but for this reason, such states are a potentially rich source of information concerning quark confinement in QCD.

The study of heavy-quark mesons is a natural starting point in the search to understand hadron formation. The Born-Oppenheimer approximation provides a compelling and clear physical picture of both conventional and hybrid heavy-quark mesons. In this talk, the evidence supporting the validity of a Born-Oppenheimer treatment of such systems was presented. The validity of the leading Born-Oppenheimer approximation in the absence of light quarks was established by a comparison of LBO level splittings with direct simulation results. Mixings induced by quark spin effects were then shown to be small, and the effects of including light sea quarks were discussed, suggesting that a handful of hybrid mesons with diameters not extending appreciably beyond 1 fm may exist as well-defined resonances in nature.

Other recent studies involving gluonic excitations were also summarized. In particular, the pure-gauge glueball masses, the light quark 1^{-+} hybrid meson mass, and the static three-quark potential and its first excitation were presented. This work was supported by the U.S. National Science Foundation under award PHY-0099450, the U.S. DOE, Grant No. DE-FG03-97ER40546, and the European Community's Human Potential Programme under contract HPRN-CT-2000-00145, Hadrons/Lattice QCD.

REFERENCES

1. D. Thompson *et al.*, Phys. Rev. Lett. **79**, 1630 (1997); G. Adams *et al.*, Phys. Rev. Lett. **81**, 5760 (1998); A. Abele *et al.*, Phys. Lett. B**423**, 175 (1998).

2. P. Hasenfratz, R. Horgan, J. Kuti, J. Richard, Phys. Lett. **B95**, 299 (1980).
3. K.J. Juge, J. Kuti, and C. Morningstar, Nucl. Phys. B(Proc. Suppl.) **63** 326, (1998); and hep-lat/9809098.
4. S. Perantonis and C. Michael, Nucl. Phys. **B347**, 854 (1990).
5. K.J. Juge, J. Kuti, and C. Morningstar, Phys. Rev. Lett. **90**, 161601 (2003).
6. G.S. Bali, K. Schilling, C. Schlichter, Phys. Rev. D **51**, 5165 (1995).
7. K.J. Juge, J. Kuti, and C. Morningstar, Phys. Rev. Lett. **82**, 4400 (1999).
8. C. Davies *et al.*, Phys. Rev. **D58**, 054505 (1998).
9. T. Burch and D. Toussaint, hep-lat/0305008.
10. G.S. Bali *et al.*, Phys. Rev. D **62**, 054503 (2000).
11. X. Liao and T. Manke, Phys. Rev. D **65**, 074508 (2002).
12. X. Liao and T. Manke, hep-lat/0210030.
13. C. Morningstar and M. Peardon, Phys. Rev. D **60**, 034509 (1999).
14. R.L. Jaffe, K. Johnson, and Z. Ryzak, Ann. Phys. **168**, 344 (1986).
15. J. Kuti, Nucl. Phys. (Proc. Suppl.) **73**, 72 (1999).
16. T. Barnes, F. Close, and S. Monaghan, Nucl. Phys. **B198**, 380 (1982).
17. C. Carlson, T. Hansson, and C. Peterson, Phys. Rev. D **27**, 1556 (1983).
18. N. Isgur and J. Paton, Phys. Rev. D **31**, 2910 (1985).
19. C. Bernard *et al.*, hep-lat/0301024.
20. H. Ichie, V. Bornyakov, T. Streuer, and G. Schierholz, Nucl. Phys. B (Proc. Suppl.) **119**, 751 (2003), *Lattice 2002: 20th International Symposium on Lattice Field Theory*, Boston, MA, 24-29 June 2002, edited by R. Edwards, J. Negele and D. Richards (North-Holland, Amsterdam) (hep-lat/0212024).
21. H. Ichie, V. Bornyakov, T. Streuer, G. Schierholz, *PANIC 02: 16th International Conference on Particles and Nuclei*, Osaka, Japan, 30 Sep - 4 Oct 2002 (hep-lat/0212036).
22. T. Takahashi and H. Suganuma, Phys. Rev. Lett. **90**, 182001 (2003).